Cardiovascular Research (2010) **85**, 631–640
doi:10.1093/cvr/cvp308

Exercise training decreases store-operated Ca^{2+} entry associated with metabolic syndrome and coronary atherosclerosis

Jason M. Edwards[1†], Zachary P. Neeb[1†], Mouhamad A. Alloosh[1], Xin Long[1], Ian N. Bratz[2], Cassandra R. Peller[1], James P. Byrd[1], Sanjay Kumar[1], Alexander G. Obukhov[1], and Michael Sturek[1*]

[1]Department of Cellular and Integrative Physiology, Indiana University School of Medicine, 635 Barnhill Drive, MS 385, Indianapolis, IN 46202-5120, USA; and [2]Department of Integrative Medical Sciences, Northeastern Ohio Universities Colleges of Medicine, OH, USA

Received 3 February 2009; revised 3 September 2009; accepted 7 September 2009; online publish-ahead-of-print 10 September 2009

Time for primary review: 21 days

Aims Stenting attenuates restenosis, but accelerated coronary artery disease (CAD) adjacent to the stent (peri-stent CAD) remains a concern in metabolic syndrome (MetS). Smooth muscle cell proliferation, a major mechanism of CAD, is mediated partly by myoplasmic Ca^{2+} dysregulation and store-operated Ca^{2+} entry (SOCE) via canonical transient receptor potential 1 (TRPC1) channels is proposed to play a key role. Exercise is known to prevent Ca^{2+} dysregulation in CAD. We tested the hypothesis that MetS increases SOCE and peri-stent CAD and exercise attenuates these events.

Methods and results Groups ($n = 9$ pigs each) were (i) healthy lean Ossabaw swine fed standard chow, (ii) excess calorie atherogenic diet fed (MetS), and (iii) aerobically exercise trained starting after 50 weeks of development of MetS (XMetS). Bare metal stents were placed after 54 weeks on diets, and CAD and SOCE were assessed 4 weeks later. Coronary cells were dispersed proximal to the stent (peri-stent) and from non-stent segments, and fura-2 fluorescence was used to assess SOCE, which was verified by Ni^{2+} blockade and insensitivity to nifedipine. XMetS pigs had increased physical work capacity and decreased LDL/HDL ($P < 0.05$), but no attenuation of robust insulin resistance, glucose intolerance, hypertriglyceridaemia, or hypertension. CAD was greater in peri-stented vs. non-stented artery segments. MetS had the greatest CAD, SOCE, and TRPC1 and STIM1 mRNA and protein expression, which were all attenuated in XMetS.

Conclusion This is the first report of the protective effect of exercise on native CAD, peri-stent CAD, SOCE, and molecular expression of TRPC1, STIM1, and Orai1 in MetS.

Keywords Transient receptor potential 1 channel • STIM1 • Orai1 • Store-operated calcium channel • Intravascular ultrasound • Coronary smooth muscle • Ossabaw miniature swine

1. Introduction

Metabolic syndrome (MetS) is defined as the combination of several risk factors including central obesity, dyslipidaemia (increased LDL/HDL and triglycerides), hypertension, impaired glucose tolerance, and insulin resistance.[1] Generally, the presence of three of these characteristics renders a diagnosis of MetS.[1] This combination of risk factors, also termed 'pre-diabetes', ultimately leads to type 2 diabetes and increased prevalence and severity of coronary artery disease (CAD).[2]

Untreated CAD will progress to the point where neointimal formation occludes coronary blood flow and impairs cardiac function. The primary interventional treatment for occlusive CAD is deployment of a coronary stent. Drug-eluting stents have substantially decreased such restenosis; however, artery segments adjacent to the stent's edge (peri-stent) are sites of significant stenosis.[3]

† These authors contributed equally to this work.

* Corresponding author. Tel: +1 317 274 7772, Fax: +1 317 274 3318, Email: msturek@iupui.edu

Accelerated peri-stent CAD progression increases the need for repeat stent procedures[3–5] and shows a greater prevalence in patients with diabetes.[6] Since peri-stent CAD may be a milder representation of in-stent restenosis due to stent-induced injury, there is need for study of the cellular and molecular mechanisms underlying peri-stent CAD.

Clearly, coronary smooth muscle (CSM) proliferation is largely responsible for neointima formation after coronary stenting.[7] Intracellular Ca^{2+} plays several roles in smooth muscle cells, such as regulation of contraction and gene expression,[8] and altered intracellular Ca^{2+} signalling is associated with smooth muscle cell proliferation.[9] The primary Ca^{2+} store within the CSM cell is the sarcoplasmic reticulum (SR). Depletion of the SR Ca^{2+} store leads to store-operated Ca^{2+} entry (SOCE) across the plasma membrane in smooth muscle.[10] SOCE [or Ca^{2+}-release-activated Ca^{2+} entry] historically has been described in purely electrophysiological terms, as the molecular entity was not known (as reviewed in Lewis[11] and Clapham[12]). In recent years, various candidates have been proposed to be involved in SOCE, including transient receptor potential canonical 1 (TRPC1), TRPC6, STIM1, and Orai1 (as reviewed in Lewis[11] and Clapham[12]). Importantly, the TRPC1 channel that contributes to SOCE in smooth muscle is linked to hypertrophy and proliferation.[8,10,13] Balloon injury-induced CSM cell proliferation in healthy juvenile swine is associated with up-regulation of TRPC1 channels.[13] In addition to pharmacological antagonism of aberrant Ca^{2+} signalling,[14] we have shown that exercise therapy prevents CSM Ca^{2+} dysregulation in CAD.[15,16] Although TRPC1 channels are strongly associated with smooth muscle proliferation and have been implicated in CAD, no studies have examined changes in TRPC1 channels in native (non-stent) and peri-stent CAD in MetS or whether exercise training can attenuate these processes.

Our group has developed Ossabaw miniature swine as an excellent large animal model of MetS.[17–20] We tested the hypothesis that MetS increases SOCE and CAD in non-stent and peri-stent segments of coronary artery and exercise attenuates these events. Our data provide the first cellular and molecular evidence that exercise protects against increases in SOCE, TRPC1, and STIM1 protein, and native and peri-stent CAD in MetS. These findings in the Ossabaw miniature swine model, which superbly mimics CAD in MetS, are critical links for translation to clinical medicine.

2. Methods

2.1 Animal care and use

All protocols involving animals were approved by an Institutional Animal Care and Use Committee and complied fully with recommendations in the Guide for the Care and Use of Laboratory Animals[21] and the American Veterinary Medical Association Panel on Euthanasia.[22] The investigation conforms with the Guide for the Care and Use of Laboratory Animals published by the US National Institutes of Health (NIH Publication No. 85-23, revised 1996). Male Ossabaw swine (aged 7 months, sexually mature) were assigned to diet

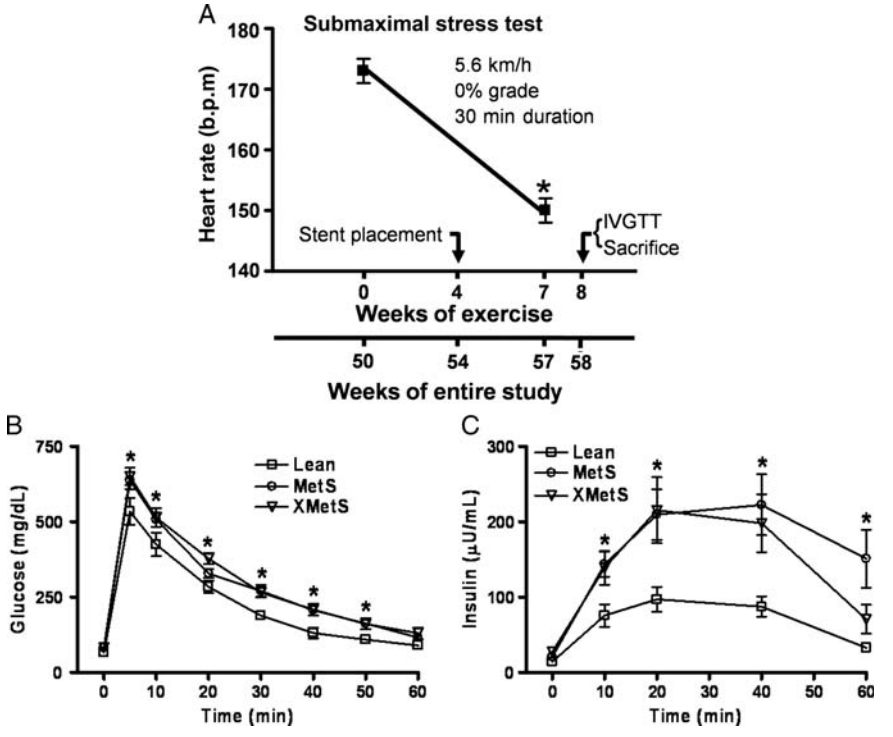

Figure 1 Ossabaw swine fed excess atherogenic diet are glucose intolerant and insulin-resistant and exercise training improves physical work capacity. (*A*) Timeframe of study treatments and exercise stress test (see Section 2). (*B*) Time course of blood glucose responses during IVGTT. (*C*) Time course of plasma insulin responses during IVGTT. $n = 7$ Lean, 8 MetS, and 8 XMetS. $^*P < 0.05$ compared to 0 weeks of exercise (*A*) or Lean (*B* and *C*).

groups for 54 weeks before stenting (*Figure 1A*). Lean control swine (Lean, $n = 9$) were fed lean chow. Sedentary MetS ($n = 9$) and exercise trained (XMetS, $n = 9$) groups were fed a high fat/2% cholesterol atherogenic diet. See Supplementary material online for detailed methods.

2.2 Exercise training

After 50 weeks of MetS development, pigs randomized to the endurance exercise group began treadmill training 4 weeks prior to stenting and continued exercise for 3–4 weeks after stenting. The training protocol was similar to our previous studies (e.g. Witczak *et al.*[15]) and guidelines.[23] See Supplemental material online for detailed methods.

2.3 Submaximal stress test

At weeks 0 and 7 of exercise training, animals underwent a submaximal stress test consisting of running on a treadmill at 5.6 km/h, 0% grade for 30 min at which point heart rate data were collected (*Figure 1A*).

2.4 Intravenous glucose tolerance test

Intravenous glucose tolerance test (IVGTT) was preformed as previously described by our laboratory.[17–19] Briefly, conscious swine acclimatized to low-stress restraint in a sling were fasted overnight and baseline blood samples were obtained. Glucose (1 g/kg body weight, iv) was administered and timed blood samples were collected.

2.5 Plasma lipid assays

Fasting blood samples were analysed for triglyceride and total cholesterol (fractionated into HDL and LDL components).[17] Cholesterol in lipoprotein fractions was determined after precipitation of HDL using minor modifications of standard methods.[24] See Supplementary material online for detailed methods.

2.6 Stent procedure

Procedures were similar to previous reports.[18,25,26] Briefly, intravascular ultrasound (IVUS) pullback was performed in the left circumflex coronary artery (CFX) where one stent was deployed in each animal. Angiography was performed to ensure proper longitudinal stent placement and IVUS was repeated to confirm deployment of the stent to the proper arterial lumen diameter (1.0× normal artery reference).[18,25,26] See Supplementary material online for detailed methods.

2.7 Intra-stent histology

Stented coronary segments were placed in zinc-buffered formalin at sacrifice for standard histological analysis.[27] See Supplementary material online for detailed methods.

2.8 Cell dispersion

The procedure for the isolation of the coronary artery and the enzymatic dispersal of CSM cells for acute use has been described previously.[9,15]

2.9 Intracellular Ca^{2+} measurements

Whole-cell intracellular Ca^{2+} levels were obtained at room temperature (22–23°C) using the fluorescent Ca^{2+} indicator, fura-2, and the InCa++ Ca^{2+} Imaging System (Intracellular Imaging, Cincinnati, OH, USA) as previously described by our laboratory.[9,14,15]

2.10 Patch-clamp electrophysiology

All electrophysiological experiments were performed using an Axopatch 200B integrating patch-clamp amplifier and a DigiData 1440A analog-digital converter and analysed using Axon PCLAMP 10 software package. Cells were voltage-clamped at a holding potential of −60 mV and 300 ms voltage ramps from −100 to +100 mV were applied at 5 s intervals similar to previous protocols.[28] See Supplementary material online for detailed methods.

2.11 Reverse transcription–polymerase chain reaction

The total RNA from pig coronary arteries was isolated using TRIzol reagent (Invitrogen, Carlsbad, CA, USA). The full-length transcripts of TRPC1 were amplified using the one-step SuperScript RT–PCR platinum *Taq* HiFi system (Invitrogen). The full transcripts were confirmed to be the pig TRPC1 by sequencing and are included in the Supplementary material online.

2.12 Real-time reverse transcription–polymerase chain reaction (or quantitative reverse transcription–polymerase chain reaction) analysis

BioRad iScript cDNA Synthesis kit was used to reverse transcribe cDNA from coronary. The Applied Biosystems 7500 Real Time PCR System was used. The endogenous control (18S rRNA) was amplified using TaqMan Universal PCR Master Mix (Applied Biosystems, Foster City, CA, USA), whereas TRPC/Orai/Stim was amplified using SYBR Green Master mix (Applied Biosystems). See Supplementary material online for detailed methods.

2.13 Immunoblots

Bound horseradish peroxidase (HRP)-conjugates [anti-rabbit or mouse HRP-conjugated antibody (Pierce, Rockford, IL, USA, 1:20 000)] were detected using a SuperSignal West Femto Kit (Pierce). The monoclonal anti-TRPC1 antibody was a gift from Dr Tsiokas (University of Oklahoma Health Sciences Center). STIM1 and ORAI1 antibodies were from Alomone labs (Rehovet, Israel). See Supplementary material online for detailed methods.

2.14 Assessment of CAD (atherosclerosis)

IVUS pullbacks performed during the stenting procedure and before stent placement were used to assess native atheroma.[16,26] Per cent circumferential wall coverage was calculated similar to previous reports.[17,26] See Supplementary material online for detailed methods.

2.15 Statistical analysis

Analysis of variance (ANOVA) with the Student–Newman–Kuels *post hoc* analysis was performed using commercially available software (SPSS 10.0 and SigmaStat 4.0) and $P < 0.05$ was the criterion for statistical significance. In an attempt to avoid a type II interpretive error (false-negative), significance was reported at $P < 0.10$ where appropriate.[29]

3. Results

To determine whether excess kilocalorie atherogenic diet induces MetS in Ossabaw swine, we evaluated the major parameters associated with MetS (*Table 1*). Several characteristics were elevated in MetS and XMetS above Lean, including body weight, LDL, systolic and diastolic blood pressure, and fasting blood glucose. LDL/HDL ratio was the only metabolic parameter attenuated by exercise training in XMetS vs. MetS. Efficacy of exercise

Table 1 Phenotypic characteristics of Ossabaw miniature swine groups at the end of study

Parameter	Lean	MetS	XMetS	Significance
Weight (kg)	64 ± 3	111 ± 9	120 ± 5	XMetS, MetS > Lean
Total cholesterol (mg/dL)	48 ± 2	215 ± 31	219 ± 6	XMetS, MetS > Lean
LDL (mg/dL)	26 ± 4	155 ± 4	136 ± 16	XMetS, MetS > Lean
HDL (mg/dL)	18 ± 3	56 ± 10	83 ± 6	XMetS, MetS > Lean
LDL/HDL	1.8 ± 0.4	3.5 ± 0.7	1.7 ± 0.2	MetS > XMetS, Lean
Triglycerides (TG, mg/dL)	25 ± 3	39 ± 1	40 ± 2	XMetS, MetS > Lean
Systolic blood pressure (mmHg)	116 ± 1	160 ± 1	146 ± 6	XMetS, MetS > Lean
Diastolic blood pressure (mmHg)	77 ± 2	108 ± 5	94 ± 7	XMetS, MetS > Lean
Fasting blood glucose	67 ± 2	83 ± 2	82 ± 2	XMetS, MetS > Lean
Resting heart rate (b.p.m.)	69 ± 3	93 ± 4	78 ± 1	MetS > XMetS > Lean
Resting heart rate start exercise training (b.p.m)	—	—	102 ± 1	End < start training
Treadmill grade at 65–75% maximum heart rate				
Start exercise training	—	—	3%	—
End exercise training	—	—	8 ± 0.3%	End > start training
Submaximal stress test heart rate (b.p.m.)				
Start exercise training	—	—	173 ± 2	—
End exercise training	—	—	150 ± 2	End < start training

Lean control; MetS, metabolic syndrome; XMetS, exercise trained MetS.

training was evidenced as decreased resting heart rate, increased work load (treadmill grade) at a constant heart rate (65–75% maximum), and decreased heart rate at a constant work load during the treadmill stress test (*Figure 1A*).

Glucose intolerance and insulin resistance are major components of MetS and the development of type 2 diabetes. MetS had significantly greater blood glucose concentrations than Lean at 10, 20, 30, 40, and 50 min after bolus glucose injection (*Figure 1B*). In addition, XMetS had significantly elevated blood glucose above Lean at 10, 30, 40, and 50 min time points (*Figure 1B*). MetS also elicited significant elevation in plasma insulin response above Lean at all times after glucose injection (*Figure 1C*). Likewise, XMetS plasma insulin was significantly elevated above Lean with the exception of the 60 min time point (*Figure 1C*). Taken together, both glucose and insulin IVGTT results indicate glucose intolerance and primary insulin resistance in MetS and XMetS, with minimal effect of this short-term (7 weeks) exercise training programme on these metabolic parameters.

To determine the effects of MetS on CAD, atherosclerosis was imaged by IVUS and quantified as per cent circumferential wall coverage. *Figure 2A* is a schematic of the coronary vasculature showing the location of peri-stent and non-stent segments studied. *Figure 2B* illustrates an *in vivo* coronary angiogram at right anterior oblique 30° angle. Representative IVUS image from the CFX artery demonstrates atherosclerotic neointima formation (*Figure 2C*). IVUS images before (*Figure 2D*) and after stent (*Figure 2E*) deployment verified proper stent diameter. Representative longitudinal IVUS analysis of CFX before and 4 weeks after stent deployment illustrates relatively mild and diffuse atherosclerosis through the more distal regions of the artery (*Figure 2F*). Increased per cent wall coverage was found in proximal and distal non-stented segments of coronary arteries in MetS compared with Lean, which was attenuated with exercise (XMetS) (*Figure 2G* and *H*). Similar to non-stent segments, exercise (XMetS) completely prevented the increase in per cent wall coverage observed in MetS compared with Lean in peri-stent segments of coronary artery (*Figure 2I*), but did not affect in-stent neointimal hyperplasia (*Figure 2J*).

Verhoff-Van Giessen, Masson's trichrome, and haematoxylin and eosin (H&E) stains were performed to assess in-stent plaque morphology. *Figure 3A* and *B* show representative in-stent plaque from trichrome and H&E, respectively. Neointimal hyperplasia was not different across groups (*Figure 3C*). Exercise reduced the amount of collagen (*Figure 3D*), but there was no difference in cell density between groups in the in-stent regions (*Figure 3E*).

Since alterations in SOCE signalling mechanisms have been associated with atherosclerosis,[8,10,13] we studied SOCE in smooth muscle cells freshly isolated from non-stent and peri-stent artery segments of Lean, MetS, and XMetS groups. To assess SOCE, we first employed a typical store-depletion protocol similar to that reviewed by Landsberg and Yuan.[10] *Figure 4A* shows a representative record of intracellular Ca^{2+} changes in a peri-stent MetS CSM cell obtained during such an experiment. Baseline intracellular [Ca^{2+}] was established from minutes 0 to 2 in physiological salt solution containing normal 2 mM Ca^{2+}. From minutes 3 to 7, the caffeine-sensitive SR Ca^{2+} stores were depleted in the presence of caffeine and the SERCA inhibitor cyclopiazonic acid (CPA) in Ca^{2+} free solution. At minutes 17–22, Ca^{2+} was reintroduced and SOCE was quantified in non-stent and peri-stent cells. CSM SOCE was sensitive to the non-selective Ca^{2+} channel blocker Ni^{2+}, but insensitive to the L-type Ca^{2+} channel blocker nicardipine. Peak SOCE was not significantly different in the CSM cells from peri-stent segments of Lean and

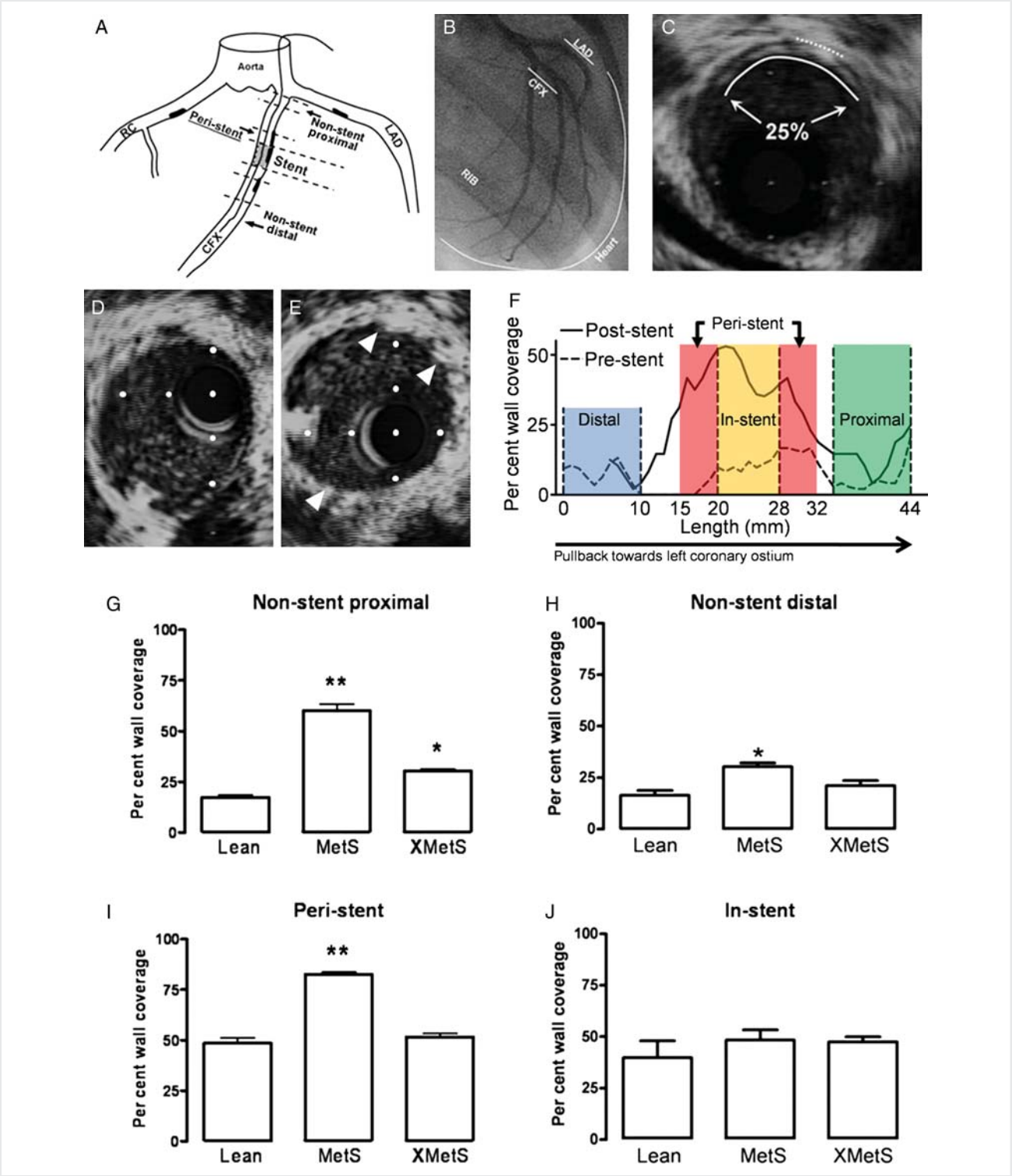

Figure 2 Greater coronary atherosclerosis in MetS swine vs. Lean is attenuated by exercise training, but in-stent neointimal hyperplasia is not affected. (*A*) Schematic of coronary vasculature. (*B*) Coronary angiogram showing CFX and its large obtuse marginal branches and the left anterior descending (LAD) coronary arteries in right anterior oblique view. (*C*) IVUS image. Dotted line indicates small section of internal elastic lamina and solid line indicates lumen boundary, showing 25% circumferential wall coverage of this cross-section of artery. Representative IVUS image of artery segment to receive stent immediately preceding stent placement in (*D*) and immediately following stent placement in (*E*) (arrowheads are stent struts). (*F*) Representative per cent wall coverage from IVUS data collected along the length of a stented artery both preceding stent placement (dotted line) and after 4 weeks recovery post-stent (solid line). (*G*) Proximal non-stent per cent wall coverage. $^{**}P < 0.05$ vs. Lean and XMetS, $^{*}P < 0.05$ vs. Lean and MetS. (*H*) Distal non-stent per cent wall coverage. $^{*}P < 0.05$ vs. Lean. (*I*) Per cent wall coverage in peri-stent segments. $^{**}P < 0.05$ vs. Lean and XMetS. (*J*) In-stent per cent wall coverage. $n = 6$ Lean, 6 MetS, and 6 XMetS.

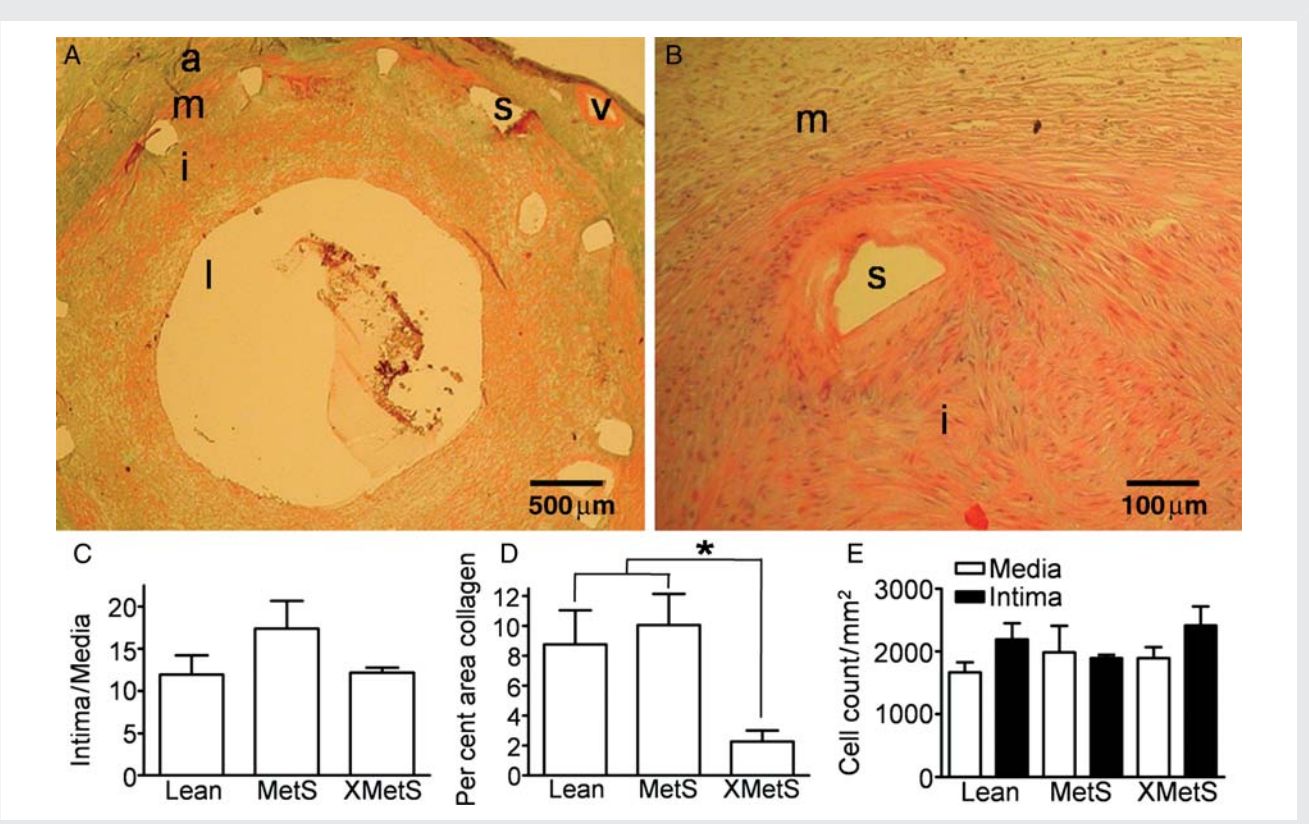

Figure 3 Intra-stent histology. (*A*) Representative trichrome section. (*B*) Representative H&E section. (*C*) Intima/media cross-sectional area. (*D*) Collagen in XMetS as a per cent of intra-stent media and intimal area. (*E*) Cellularity (H&E section) in media and intima. a, adventitia; m, media; i, intima; l, lumen; s, stent; v, vasa vasorum. $n = 7$ Lean, 4 MetS, and 5 XMetS. $^*P < 0.05$ XMetS vs. Lean and MetS.

MetS in Ca^{2+} imaging experiments, but was markedly attenuated in XMetS (*Figure 4B*).

In a separate chronic study, SOCE was evaluated by Mn^{2+} quench in cells of non-stent and peri-stent segments. An Mn^{2+}-dependent decrease in the fluorescence intensity of fura-2 excited at 360 nm (the fura-2 Ca^{2+}-insensitive isosbestic point) is indicative of divalent cation influx. Caffeine and CPA were used to deplete intracellular Ca^{2+} stores in CSM cells. Mn^{2+} quench confirmed that store-depletion resulted in divalent cation influx sensitive to the non-selective Ca^{2+} channel blocker Ni^{2+} (*Figure 4C*). Mn^{2+} influx was significantly greater in MetS compared with Lean in both non-stent and peri-stent cells (*Figure 4D*).

A less extreme Ca^{2+} store-depletion protocol using caffeine alone in the absence of CPA demonstrated significant Mn^{2+} quench (*Figure 4E*), which was greater in MetS compared with the Lean group (*Figure 4F*). Mn^{2+} quench observed in *Figure 4D* and *F* confirmed that store-depletion results in divalent cation influx in CSM cells without inhibition of SERCA. Whole-cell patch-clamp electrophysiology was performed using a protocol similar to *Figure 4E*. Caffeine-induced inward current was sustained for >5 min (*Figure 4G*), indicating that it was not due to transient Ca^{2+}-sensitive Cl^- channels activated by Ca^{2+}-release stimulated by caffeine. A current–voltage relationship plot of the sustained inward current was ohmic with a reversal potential of ~ 0 mV (*Figure 4H*).

Although our patch-clamp data suggested that SOCE was due to TRPC1, we determined whether changes in the molecular expression of TRPC1 or other SOCE-related proteins (e.g. STIM1 and Orai1) could account for the increased SOCE. In reverse transcription–polymerase chain reaction (RT–PCR) experiments, the presence of TRPC1, STIM1, and Orai1 was shown in all groups (*Figure 5A–D*). Group data demonstrated significantly greater TRPC1 mRNA expression in the MetS group compared with Lean, which was attenuated by exercise training (*Figure 5B*). STIM1 and Orai1 mRNA expression were also increased in the MetS group, but remained increased even with exercise (*Figure 5C* and *D*). Immunoblots from coronary lysates showed that TRPC1 protein in MetS was attenuated in XMetS and STIM1 protein in MetS was abolished in XMetS compared with Lean (*Figure 5F* and *G*), whereas Orai1 protein expression shows no overall statistical difference by ANOVA between the three groups ($P = 0.10$, *Figure 5H*). Agarose gel images demonstrate the expression of only TRPC1 and TRPC6 genes in MetS coronary arteries (*Figure 5I* and *J*). TRPC6 mRNA was increased in MetS compared with Lean (*Figure 5K*).

4. Discussion

The novel findings of this study are: (i) exercise decreases (a) non-stent and peri-stent CAD, (b) store-operated Ca^{2+}

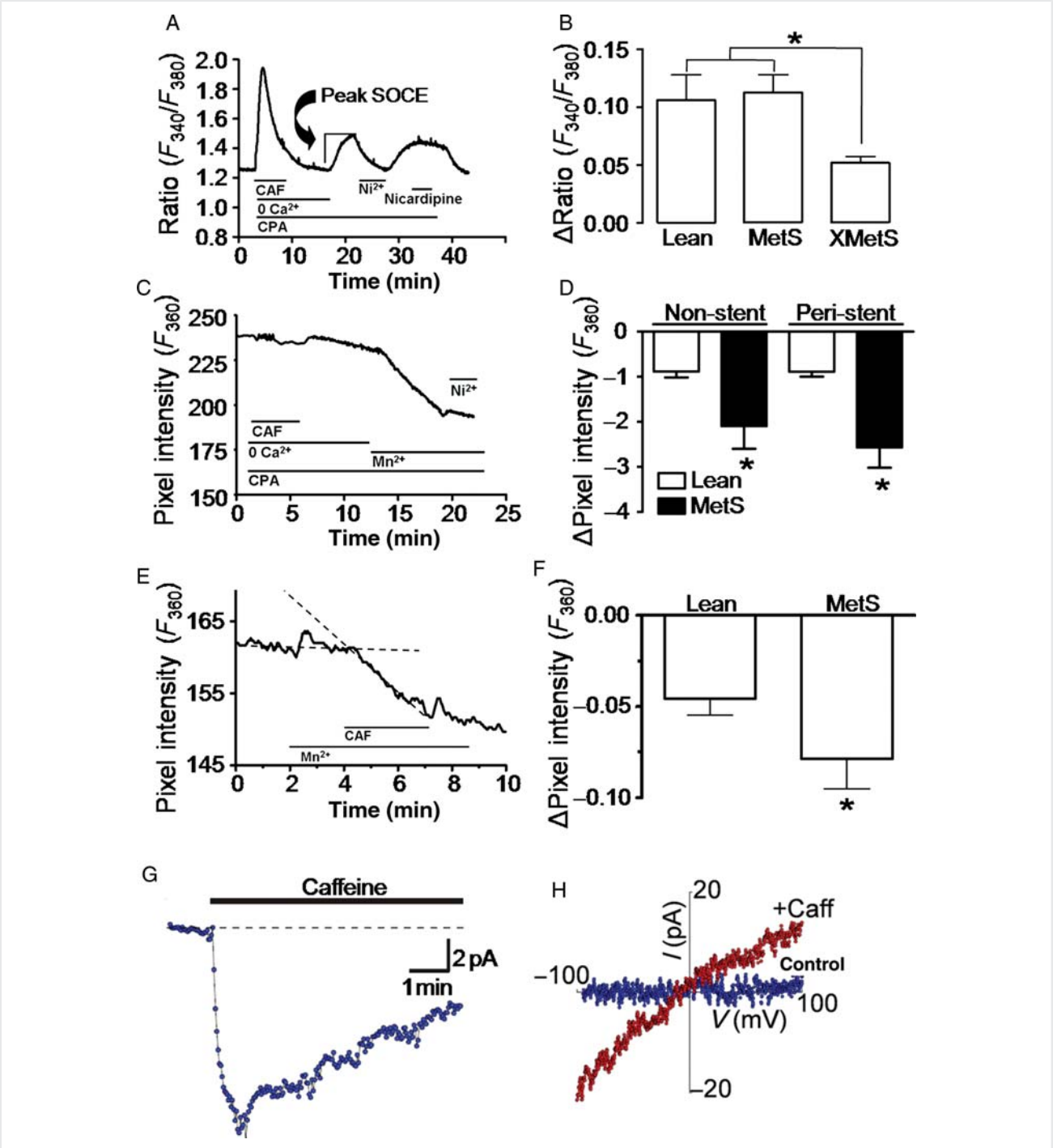

Figure 4 SOCE is increased in MetS and attenuated by exercise. (*A* and *C*) Representative data from standard protocols used to assess SOCE. Peak store-depletion-mediated Ca^{2+} influx is assessed at minutes 17–20. Duration of exposure to solutions is shown by horizontal lines; caffeine (CAF, 5 mM); cyclopiazonic acid (CPA, 10 μM). (*B*) Exercise attenuates peak SOCE compared with Lean and MetS in peri-stent sections of artery. Lean (90 cells), MetS (24 cells), and XMetS (20 cells). *$P < 0.05$ XMetS vs. Lean and MetS. (*C*) Mn^{2+} as a Ca^{2+} surrogate quenches fura-2 fluorescence at the isosbestic (Ca^{2+}-insensitive) 360 nm wavelength verifying divalent cation influx. (*D*) Increased SOCE in CSM from non-stent and peri-stent MetS coronary arteries compared with Lean. Lean (28 cells) and MetS (12 cells). *$P < 0.05$ vs. Lean. (*E*) Only caffeine is used to deplete the Ca^{2+} store in this SOCE protocol. (*F*) Increased SOCE in CSM from MetS swine. Lean (37 cells) and MetS (51 cells). *$P < 0.05$ vs. Lean. (*G*) Whole-cell patch-clamp data demonstrate sustained inward current by caffeine. (*H*) Current–voltage relationship of leak subtracted control (blue) and SOCE (red). $n = 5$ cells (Lean and MetS). $n = 5$ Lean, 4 MetS, and 4 XMetS.

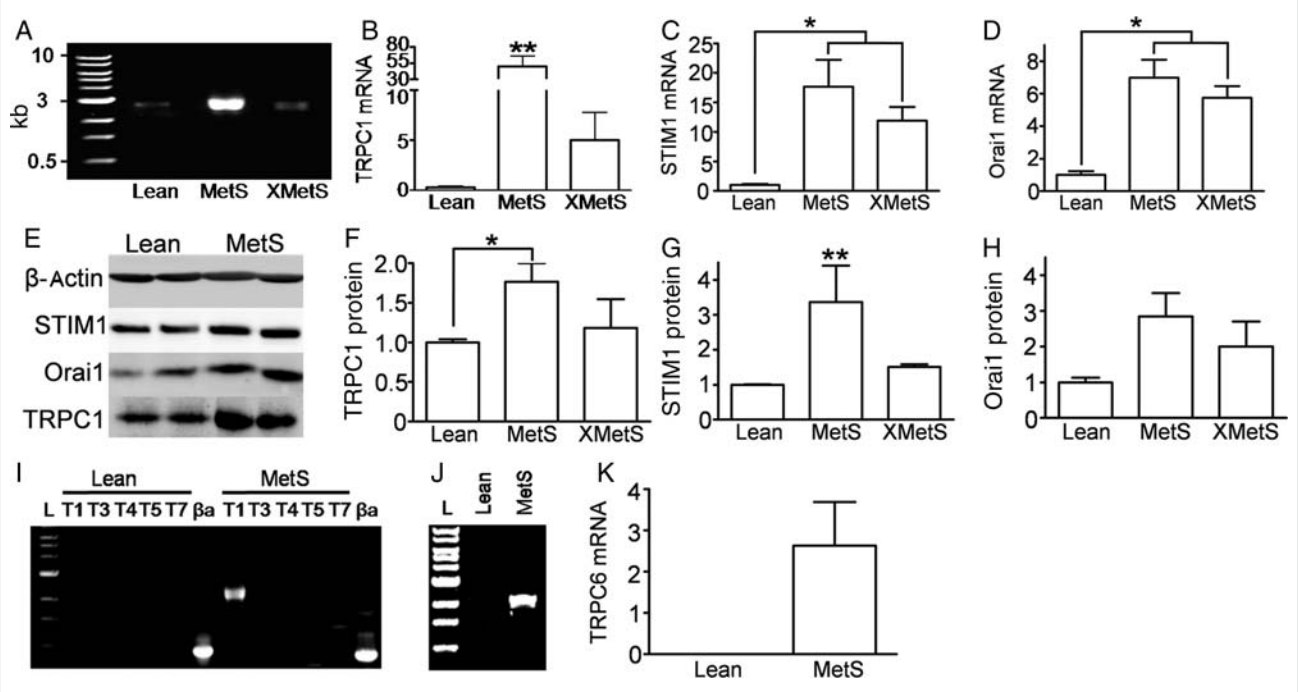

Figure 5 Increased TRPC1 and STIM1 in MetS are abolished by exercise. (*A*) Representative agarose gel image quantifying TRPC1 mRNA using RT–PCR. (*B*) TRPC1 mRNA normalized to x-actin. STIM1 (*C*) and Orai1 (*D*) mRNA using quantitative RT–PCR normalized to x-actin. (*E*) Immunoblot using anti-x-actin, STIM1, Orai1, and TRPC1 in Lean and MetS. (*F–H*) TRPC1 (*F*), STIM1 (*G*), and Orai1 (*H*) protein expression using immunoblot analysis normalized to x-actin; ANOVA $P = 0.10$ for (*H*). (*I*) Representative agarose gel image illustrating TRPC1 expression and no TRPC3, TRPC4, TRPC5, or TRPC7 expression. (*J*) Agarose gel image illustrating TRPC6 expression in MetS coronary arteries. (*K*) TRPC6 mRNA in MetS coronary arteries. $^{**}P < 0.05$ MetS compared with Lean and XMetS; $^{*}P < 0.05$ between bracketed groups. $n = 6$ for Lean, MetS, and XMetS.

channel function and TRPC1/STIM1 molecular expression, and (c) in-stent collagen content in MetS and (ii) SOCE current–voltage relationship in CSM is ohmic and non-selective, which is consistent with TRPC1. Excess kilocalorie atherogenic diet elicited robust MetS, which accompanied greater atherosclerosis in peri-stent segments of coronary arteries than in non-stented arteries. Functional store-depletion-mediated Ca^{2+} influx and TRPC1/STIM1 molecular expression were associated with the extent of atherosclerosis among groups, whereas Orai1 protein expression did not change. The effect of exercise to attenuate progression of peri-stent CAD, but not in-stent stenosis, in Ossabaw miniature swine with MetS is consistent with the clinical study in humans by Belardinelli *et al.*[5] and non-diabetic swine.[30] Our Ca^{2+} signalling and molecular expression data provide evidence of cellular and molecular events underlying this vitally important clinical phenomenon and extend those findings[5,30] to MetS.

Patient complication following stent deployment is well documented[31] with diabetes increasing patient risk.[32] Consistent with human data, MetS Ossabaw swine displayed increased atherosclerosis in non-stent artery segments compared with Lean. Peri-stent CAD has been observed by several groups and is more prevalent in patients with diabetes;[6] which may be due to the overall greater diffuse CAD in MetS and diabetes.[33] Despite this remarkable clinical observation, no studies have examined mechanisms which underlie peri-stent atherosclerosis in MetS. Similar to previous findings, peri-stent atherosclerosis, although augmented in all groups, mirrored non-stent atherosclerosis in that it was greater in MetS than Lean. Exercise has an independent role in primary prevention of CAD,[34,35] reduction of coronary stenosis, and rates of hospital readmission after coronary angioplasty.[5] Nonetheless, mechanisms which underlie these changes are unclear. In the present study, 7 weeks of exercise training attenuated the increased non-stent atherosclerosis and abolished increased peri-stent atherosclerosis observed in MetS. Although 20 weeks of exercise training of non-diabetic swine attenuated neointimal hyperplasia, i.e. progression to stenosis, after angioplasty balloon-induced injury,[30] in the present study, MetS and the shorter training duration (7 weeks) are key differences that may have minimized the protective effects of exercise.

Our group captured feral swine from Ossabaw Island, GA, USA, which naturally developed a thrifty genotype in response to the evolutionary selection pressure of seasonal shortages of food.[18] When fed excess calorie atherogenic diet, Ossabaw swine develop MetS similar to humans.[17–20] Also, MetS Ossabaw swine, like humans (but different from many other laboratory animal models), develop CAD. Consistent with these findings, male Ossabaw swine in this study show increased body weight, plasma LDL, LDL/HDL ratio, and triglyceride, systolic and diastolic pressure, and heart rate. A major extension of this work is our

finding that short-term exercise training reverses the elevated LDL/HDL ratio observed in MetS.

Obese, MetS Ossabaw swine showed classical cardiovascular adaptations to exercise training, including increased physical work capacity, resting bradycardia, and decreased heart rate response to a submaximal exercise stress test, indicating efficacy of the exercise programme. The lack of exercise attenuation of other MetS characteristics is somewhat surprising, since exercise is a first-line treatment for pre-diabetes/MetS.[36] Factors may have mitigated the typical effects of exercise on MetS characteristics in Ossabaw swine. First, our study design was to maintain the atherogenic diet and obesity of the pigs, unlike the typical exercise training regimen and that in human clinical studies, in which diet improvements are also implemented.[36] Secondly, Ossabaw miniature swine have a loss-of-function mutation in the AMP kinase x3 subunit in skeletal muscle, which is a pivotal enzyme in fatty acid oxidation and glucose uptake.[37] Exercise is not as effective in activating AMP kinase in pigs having the mutation; thus, the full benefit of exercise on skeletal muscle metabolism might not be seen in Ossabaw miniature swine.[37]

Because of the widely reported occurrence of SOCE and distribution of TRPC channels in numerous cell types, including vascular cells,[38] it might be considered dogma that SOCE and TRPC channels should be abundant in CSM and regulate Ca^{2+} signalling and contraction under normal conditions. We emphasize that we have never found activation of SOCE in Yucatan swine 'healthy' CSM,[15,39] despite robust SOCE in coronary endothelial cells.[40] However, previous studies report increased expression of TRPC1 in diseased vascular smooth muscle cells.[10,13] The results of our study are in agreement with the concept that TRPC1 channels are strongly associated with CAD, as shown by increased TRPC1 mRNA and protein expression, as well as the ohmic and non-selective current–voltage relationship of SOCE in CSM consistent with current expected of TRPC1 channel.[41] TRPC6 and Orai1, known SOCE mediators, expression is increased with MetS; however, both TRPC6[42] and Orai1[43] have distinct and vastly different current–voltage relationships than those observed in this study. Although STIM1 protein expression mirrors that of TRPC1, STIM1 operates as a sensor of the intracellular Ca^{2+}-store and not as a distinct functional ion channel.[44] Additionally, TRPC1 protein is proportional to function, i.e. Ca^{2+} influx (*Figures 4* and *5*). We can largely rule out other TRPC isoforms, because they are not expressed in coronary artery[45] (*Figure 5I*). The present study further extends our knowledge concerning the role of TRPC1 by the novel finding that metabolic syndrome increases SOCE and TRPC1 expression in conjunction with CAD, all of which are attenuated by exercise training.

Our findings indicate that TRPC1 is closely associated with neointimal hyperplasia, not only in non-stent, but also in peri-stent, segments of coronary artery. This is important because neointimal hyperplasia in non-stented segments is considered a natural progression of disease, whereas peri-stent atherosclerosis may be considered an arterial response to injury.[46,47] Together, these data suggest that TRPC1 channels play a fundamental role promoting atherosclerosis in both non-stent and peri-stent segments of coronary artery. Thus, inhibition of TRPC1 channels may serve as a possible therapeutic target for the treatment of CAD. The concept of exercise and TRPC1 as potential therapeutic modes and targets is especially important because of the recent finding that treatment of conventional risk factors such as hyperglycaemia had negligible effects on prevention of cardiovascular disease in type 2 diabetic humans and had detrimental side effects.[48]

In conclusion, our data support the hypothesis that Ossabaw swine with robust MetS have increased SOCE and CAD in non-stent and peri-stent segments of coronary artery and exercise attenuates these events. Further, increased TRPC1/STIM1 protein expression was attenuated by exercise. The implications are that in human patients with metabolic syndrome who undergo coronary stenting and have attenuated peri-stent CAD with exercise training, underlying cellular events may involve TRPC1 channels and STIM1. Future studies will focus on establishing a causative role of TRPC1 channels in the progression of CAD in *ex vivo* and *in vivo* models.

Supplementary material

Supplementary material is available at *Cardiovascular Research* online.

Acknowledgements

We thank Dr Tsiokas for his generous contribution of monoclonal TRPC1 antibody, Alice Nakatsuka and Gouqing Hu for RT–PCR analysis, and Keith L. March for use of the Research Animal Angiography Laboratory of the Indiana Center for Vascular Biology and Medicine.

Conflict of interest: none declared.

Funding

This work was supported by the National Institutes of Health grant numbers HL062552 and RR013223 to M.S, HL083381 to A.G.O., the Purdue-Indiana University Comparative Medicine Program, and the Fortune-Fry Ultrasound Research Fund of the Department of Cellular and Integrative Physiology at Indiana University School of Medicine. J.M.E. and Z.P.N. are the recipients of a Translational Research Fellowship from the Indiana University School of Medicine and Z.P.N. was the recipient of a Translational Fellowship from NIH UL1 RR025761.

References

1. Eckel RH, Kahn R, Robertson RM, Rizza RA. Preventing cardiovascular disease and diabetes: a call to action from the American Diabetes Association and the American Heart Association. *Circulation* 2006;**113**:2943–2946.
2. Ford ES. Risks for all-cause mortality, cardiovascular disease, and diabetes associated with the metabolic syndrome: a summary of the evidence. *Diabetes Care* 2005;**28**:1769–1778.
3. Angiolillo DJ, Sabata M, Alfonso F, Macaya C. 'Candy wrapper' effect after drug-eluting stent implantation: deja vu or stumbling over the same stone again? *Catheter Cardiovasc Interv* 2004;**61**:387–391.
4. Sturek M, Reddy HK. Editorial: new tools for prevention of restenosis could decrease the 'oculostento' reflex. *Cardiovasc Res* 2002;**53**:292–293.
5. Belardinelli R, Paolini I, Cianci G, Piva R, Georgiou D, Purcaro A. Exercise training intervention after coronary angioplasty: the ETICA trial. *J Am Coll Cardiol* 2001;**37**:1891–1900.
6. Finn AV, Palacios IF, Kastrati A, Gold HK. Drug-eluting stents for diabetes mellitus: a rush to judgment? *J Am Coll Cardiol* 2005;**45**:479–483.
7. Farb A, Sangiorgi G, Carter AJ, Walley VM, Edwards WD, Schwartz RS *et al*. Pathology of acute and chronic coronary stenting in humans. *Circulation* 1999;**99**:44–52.

8. Takahashi Y, Watanabe H, Murakami M, Ohba T, Radovanovic M, Ono K *et al*. Involvement of transient receptor potential canonical 1 (TRPC1) in angiotensin II-induced vascular smooth muscle cell hypertrophy. *Atherosclerosis* 2007;**195**: 287–296.
9. Hill BJF, Katwa LC, Wamhoff BR, Sturek M. Enhanced endothelin$_A$ receptor-mediated calcium mobilization and contraction in organ cultured porcine coronary arteries. *J Pharmacol Exp Ther* 2000;**295**:484–491.
10. Landsberg JW, Yuan JX. Calcium and TRP channels in pulmonary vascular smooth muscle cell proliferation. *News Physiol Sci* 2004;**19**:44–50.
11. Lewis RS. The molecular choreography of a store-operated calcium channel. *Nature* 2007;**446**:284–287.
12. Clapham DE. Calcium signaling. *Cell* 2007;**131**:1047–1058.
13. Kumar B, Dreja K, Shah SS, Cheong A, Xu SZ, Sukumar P *et al*. Upregulated TRPC1 channel in vascular injury in vivo and its role in human neointimal hyperplasia. *Circ Res* 2006;**98**:557–563.
14. Wamhoff BR, Dixon JL, Sturek M. Atorvastatin treatment prevents alterations in coronary smooth muscle nuclear Ca^{2+} signaling associated with diabetic dyslipidemia. *J Vasc Res* 2002;**39**:208–220.
15. Witczak CA, Wamhoff BR, Sturek M. Exercise training prevents Ca^{2+} dysregulation in coronary smooth muscle from diabetic dyslipidemic Yucatan swine. *J Appl Physiol* 2006;**101**:752–762.
16. Mokelke EA, Dietz NJ, Eckman DM, Nelson MT, Sturek M. Diabetic dyslipidemia and exercise affect coronary tone and differential regulation of conduit and microvessel K^+ current. *Am J Physiol Heart Circ Physiol* 2005;**288**:H1233–H1241.
17. Dyson M, Alloosh M, Vuchetich JP, Mokelke EA, Sturek M. Components of metabolic syndrome and coronary artery disease in female Ossabaw swine fed excess atherogenic diet. *Comp Med* 2006;**56**:35–45.
18. Sturek M, Alloosh M, Wenzel J, Byrd JP, Edwards JM, Lloyd PG *et al*. Ossabaw Island miniature swine: cardiometabolic syndrome assessment. In: Swindle MM, ed. *Swine in the Laboratory: Surgery, Anesthesia, Imaging, and Experimental Techniques*. 2nd ed. Boca Raton: CRC Press; 2007. p397–402.
19. Bratz IN, Dick GM, Tune JD, Edwards JM, Neeb ZP, Dincer UD *et al*. Impaired capsaicin-induced relaxation of coronary arteries in a porcine model of the metabolic syndrome. *Am J Physiol Heart Circ Physiol* 2008;**294**:H2489–H2496.
20. Lee L, Alloosh M, Saxena R, Van Alstine W, Watkins BA, Klaunig JE *et al*. Nutritional model of steatohepatitis and metabolic syndrome in the Ossabaw miniature swine. *Hepatology* 2009;**50**:56–67.
21. National Research Council. *Guide for the care and use of laboratory animals*. Washington, DC: National Academy Press; 1996.
22. Beaver BV, Reed W, Leary S, McKiernan B, Bain F, Schultz R *et al*. 2000 Report of the AVMA panel on euthanasia. *JAMA* 2001;**218**:669–696.
23. Committee to Develop a Resource Book for Animal Exercise Protocols, Sturek M. *Resource Book for the Design of Animal Exercise Protocols*. Bethesda, MD: American Physiological Society; 2006.
24. Warnick G, Benderson J, Albers JJ. Dextran sulfate-Mg^{2+} precipitation procedure for quantitation of HDL cholesterol. *Clin Chem* 1982;**28**:1379–1388.
25. Edwards JM, Alloosh M, Long X, Dick GM, Lloyd PG, Mokelke EA *et al*. Adenosine A_1 receptors in neointimal hyperplasia and in-stent stenosis in Ossabaw miniature swine. *Coron Artery Dis* 2008;**19**:27–31.
26. Lloyd PG, Sheehy AF, Edwards JM, Mokelke EA, Sturek M. Leukemia inhibitory factor is upregulated in coronary arteries of Ossabaw miniature swine after stent placement. *Coron Artery Dis* 2008;**19**:217–226.
27. Dixon JL, Shen S, Vuchetich JP, Wysocka E, Sun G, Sturek M. Increased atherosclerosis in diabetic dyslipidemic swine: protection by atorvastatin involves decreased VLDL triglycerides but minimal effects on the lipoprotein profile. *J Lipid Res* 2002;**43**:1618–1629.
28. Graier WF, Simecek S, Bowles DK, Sturek M. Heterogeneity of caffeine- and bradykinin-sensitive Ca^{2+} stores in vascular endothelial cells. *Biochem J* 1994; **300**:637–641.
29. Williams JL, Hathaway CA, Kloster KL, Layne BH. Low power, type II errors, and other statistical problems in recent cardiovascular research. *Am J Physiol Heart Circ Physiol* 1997;**42**:H487–H493.
30. Fleenor BS, Bowles DK. Exercise training decreases the size and alters the composition of the neointima in a porcine model of percutaneous transluminal coronary angioplasty (PTCA). *J Appl Physiol* 2009;**107**:937–945.
31. Antoniucci D, Valenti R, Santoro GM, Bolognese L, Trapani M, Cerisano G *et al*. Restenosis after coronary stenting in current clinical practice. *Am Heart J* 1998; **135**:510–518.
32. Hammoud T, Tanguay JF, Bourassa MG. Management of coronary artery disease: Therapeutic options in patients with diabetes. *J Am Coll Cardiol* 2000;**36**:355–365.
33. Morgan KP, Kapur A, Beatt KJ. Anatomy of coronary disease in diabetic patients: an explanation for poorer outcomes after percutaneous coronary intervention and potential target for intervention. *Heart* 2004;**90**:732–738.
34. Lee IM, Sesso HD, Oguma Y, Paffenbarger RS Jr. Relative intensity of physical activity and risk of coronary heart disease. *Circulation* 2003;**107**:1110–1116.
35. Berlin JA, Colditz GA. A meta-analysis of physical activity in the prevention of coronary heart disease. *Am J Epidemiol* 1990;**132**:612–628.
36. Diabetes Prevention Program Research Group. Reduction in the incidence of type 2 diabetes with lifestyle intervention or metformin. *N Engl J Med* 2002; **346**:393–403.
37. Andersson L. Identification and characterization of AMPKg3 mutations in the pig. *Biochem Soc Trans* 2003;**31**:232–235.
38. Nilius B, Owsianik G, Voets T, Peters JA. Transient receptor potential cation channels in disease. *Physiol Rev* 2007;**87**:165–217.
39. Sturek M, Stehno-Bittel L, Obye P. Modulation of ion channels by calcium release in coronary artery smooth muscle. In: Sperelakis N, ed. *Electrophysiology and Ion Channels of Vascular Smooth Muscle Cells and Endothelial Cells*. New York: Elsevier; 1991. p65–79.
40. Graier WF, Simecek S, Sturek M. Cytochrome P450 mono-oxygenase-regulated signalling of Ca^{2+} entry in human and bovine endothelial cells. *J Physiol (Lond)* 1995;**482**:259–274.
41. Cheng KT, Liu X, Ong HL, Ambudkar IS. Functional requirement for Orai1 in store-operated TRPC1-STIM1 channels. *J Biol Chem* 2008;**283**:12935–12940.
42. Mani BK, Brueggemann LI, Cribbs LL, Byron KL. Opposite regulation of KCNQ5 and TRPC6 channels contributes to vasopressin-stimulated calcium spiking responses in A7r5 vascular smooth muscle cells. *Cell Calcium* 2009;**45**:400–411.
43. Frischauf I, Muik M, Derler I, Bergsmann J, Fahrner M, Schindl R *et al*. Molecular determinants of the coupling between STIM1 and Orai channels: differential activation of Orai1,2,3 channels by a STIM1 coiled-coil mutant. *J Biol Chem* 2009;**284**: 21696–21706.
44. Mercer JC, Dehaven WI, Smyth JT, Wedel B, Boyles RR, Bird GS *et al*. Large store-operated calcium selective currents due to co-expression of Orai1 or Orai2 with the intracellular calcium sensor, Stim1. *J Biol Chem* 2006;**281**: 24979–24990.
45. Hu G, Oboukhova EA, Kumar S, Sturek M, Obukhov AG. Canonical transient receptor potential channels expression is elevated in a porcine model of metabolic syndrome. *Mol Endocrinol* 2009;**23**:689–699.
46. Lafont A, Guzman LA, Whitlow PL, Goormastic M, Cornhill JF, Chisolm GM. Restenosis after experimental angioplasty. *Circ Res* 1995;**76**:996–1002.
47. Post MJ, Borst C, Kuntz RE. The relative importance of arterial remodeling compared with intimal hyperplasia in lumen renarrowing after balloon angioplasty. A study in the normal rabbit and the hypercholesterolemic Yucatan micropig. *Circulation* 1994;**89**:2816–2821.
48. Dluhy RG, McMahon GT. Intensive glycemic control in the ACCORD and ADVANCE Trials. *N Engl J Med* 2008;**358**:2630–2633.